2021 IEEE International Conference on Robotics and Automation (ICRA 2021)
May 31 - June 4, 2021, Xi'an, China

Evaluation of a drone-based camera calibration approach for hard-to-reach cameras

Domitille Commun[1], Cédric Pradalier[2], Michael Balchanos[1], Olivia Fischer[1] and Dimitri Mavris[1]

Abstract— **Several applications of video rely on camera calibration, a key enabler towards the measurement of metric parameters from images. Existing calibration methods have not been adapted for use with cameras that are hard to reach such as security cameras. This paper presents a drone-based camera calibration technique for the calibration of cameras in a broader range of operating environments. The technique is enabled by the use of a drone that is equipped with location sensors. In the proposed approach, the drone is used to sample points in the 3D space and its detection on the images provides the 2D matching points enabling the calibration. To design a flight path that allows for an accurate calibration, the paper proposes a methodology to evaluate the impact of path parameters and drone localization and detection uncertainties on the calibration uncertainty. This methodology is applied to evaluate the performance of different sampling paths for the calibration of a large diversity of cameras for the purpose of recommending reliable path parameters.**

I. Introduction

The growing use of video cameras for the purposes of safety, manufacturing, building construction and 3D reconstruction of objects has led to the increased use of computer vision techniques, which in turn enable the automated measurement of attributes of interest. Obtaining accurate measurement information in this way requires that cameras be calibrated [1].

Camera calibration is the determination of two sets of unknown parameters, intrinsic and extrinsic parameters, that are used to compute the transformations that map 3D points to their 2D image. Camera calibration processes typically start by determining a training set of 3D points and their matching 2D points [2]. These key points are then used as the inputs to an optimization method that aims at minimizing the mean squared error between the actual coordinates of the 2D key points and the ones predicted by the model, the latter being functions of the unknown parameters and the 3D key points [3]. By minimizing this function, an estimate of the unknown parameters is obtained and used to build the mapping that relates 3D to 2D points.

Desired applications requiring calibration include vehicle speed measurements for safety applications or the location of obstacles in 3D, such as electrical poles, for Urban Air Mobility (UAM) applications. In 2018, there were 70 million security cameras installed in the United-States [4], but most of them are not calibrated. As an example, the Georgia Tech campus of Atlanta has more than 2,000 security cameras that are installed and operated, but not calibrated. Enabling their calibration would make the measurement of vehicle or pedestrian speed and the locating of obstacles possible and could help improve safety. These cameras are already installed and sometimes located in remote locations, which makes the current calibration approaches unsuitable. This paper presents a calibration approach that relies on the use of a drone to collect data that enables the calibration of such cameras.

Current calibration techniques can be divided into two groups: object-based calibration and self-calibration. The first group of techniques uses an object of known geometry in order to gather 3D points and their corresponding 2D points to build the mapping from 3D to 2D [5]. Three types of methods were developed to enable object-based camera calibration. The first method uses a 3D object with two or three orthogonal planes. The second one, developed by Zhang [6], uses a planar pattern that is moved in front of the camera at different orientations to obtain the camera parameters and calibrate the camera. The third alternative solution for object-based calibration relies on the use of a 1D object such as a wand that is moved in front of the camera [5]. These three methods require the use of an object that can cover the camera field of view (FOV). However, if only part of the field of view is covered by the object, then the calibration results in poor accuracy [7]. Security cameras' fields of view are large, which make handheld object-based calibration methods unsuitable. In [8], a calibration method is presented that enables calibration of cameras in a large variety of situations including when the camera field of view is large. However, the method is tedious to set up for large fields of view or cameras that are difficult to reach since it requires taking several images of a calibration grid while ensuring that the sets of images overlap and cover the entire image region. In [7], a method that enables calibration of the image-to-ground homography for security cameras is presented. The method requires the use of a small calibration board that is moved on the ground to cover the entire field of view. For each small area on the ground covered by the planar pattern the homography is computed and from it a global homography is determined. This method is tedious since it requires the use of a small calibration object that is moved on the large field of view. Although these object-based calibration methods successfully enable calibration, the tedious elements required for the calibration of security cameras – and other cameras

[1] Aerospace Systems Design Laboratory, Georgia Tech, Atlanta, USA (e-mail: dcommun3@gatech.edu).
[2]CNRS UMI 2958, Georgia Tech Lorraine, France

that are difficult to reach – significantly detract from their usability.

The second set of techniques is called self-calibration and relies on the information contained in the image to determine the camera parameters [9]. These techniques rely on constraints imposed on the camera motion or on the scene, which make them not adapted to calibrate cameras in a large variety of environments [10].

This paper proposes to use a drone and its observation in images to collect 3D and 2D data points, hence allowing for cameras to be calibrated independently of their environment or field of view size. Camera calibration depends on the availability of pairs of matching 3D points with their 2D observation in the image plane. The uncertainty in the measurement of these points translates into uncertainty in the resulting calibration [11, 6]. When using a drone as a 3D object and an automated approach to detect it in the image, the calibration is impacted by the drone path as well as the uncertainty in the drone 3D localization and the uncertainty in the localization of the drone in the image plane. The main contribution of this paper is to propose a methodology to estimate the uncertainty resulting from a given path of the drone, the localization and detection uncertainties and the camera parameters. Using this methodology, a survey that links a wide diversity of cameras with 3D point sampling parameters is designed. This allows us to highlight the influence of various path parameters on the calibration reliability expressed as the expected Root-Mean-Square reprojection error. We also show how our methodology lets us recommend reliable path parameters for known cameras.

The paper is organized as follows: section II provides an overview of the proposed methodology to evaluate calibration uncertainty resulting from a path, and localization and detection uncertainties. The approach is developed and tested within experiments described in section III. Section IV presents the results of the experiments and section V provides final conclusions and outlines potential opportunities for future research.

II. PROPOSED APPROACH

A. Calibration principle, assumptions and notations

In this paper, we assume that the camera is calibrated using a black-box method that computes the camera intrinsic and extrinsic parameters C using a set of n pairs of 3D points P_i with their corresponding observation p_i in the image plane. We do not specify the calibration method, but we assume it is able to provide a reprojection function h(P_i,C), which produces a predicted pixel observation $\tilde{p}_i$. The Root-Mean-Square (RMS) reprojection error is then

$$E(C)=\sqrt{\frac{1}{n}\sum_{i=1}^{n}\|p_i - h(P_i, C)\|^2} \quad (1)$$

The uncertainties on the 3D points and 2D points are assumed Gaussian, with zero mean and covariances $S_i Id_3$ and $s_i Id_2$ respectively.

B. Calibration uncertainty

Most calibration techniques are based on complex non-linear optimization [3]. As a result, the theoretical prediction of the calibration uncertainty is reliable for small noise levels on the image only [12]. Instead, we propose to evaluate the calibration uncertainty and reliability through an estimation of the statistics of the RMS reprojection error. To this end, inspired by approaches described in [12, 6], we use the Monte-Carlo sampling presented in the following algorithm:

Pseudo-code

Repeat k times:
  For i in $[1, n]$:
    Draw Q_i from a normal distribution $N(P_i, S_i Id_3)$
    Draw q_i from a normal distribution $N(p_i, s_i Id_2)$
  Estimate C using the selected calibration method
  Compute and store E(C) as E_k(C)
Compute statistics on the set of measurements E_k(C): mean, max, variance...

The proposed algorithm is interesting because it can highlight the variability and reliability of the calibration results for the selected set of 3D points. In comparison with traditional calibration methods where the calibration target geometry is well known, this better represents the challenges faced when using a moving agent with a less certain localization.

The choice of k was set to 500 after observing the convergence of the Monte Carlo estimator for various cameras. Starting from 500 iterations, the amplitude of the oscillations of the estimator is decreased by 90% percent compared to the amplitudes for a small number of iterations. Figure 1 illustrates this trend for a camera with focal length of 1,000 pixels and image width and height of 1,200 pixels. Beyond this number of iterations, the gain in precision of the estimator was not worth the additional computation time.

C. Survey of the relation between path sampling parameters and calibration statistics

Given a camera, the long-term purpose of this research is to design a flight path for a drone and to use the observation of this path to estimate the camera parameters. However, before tackling this challenge, a simulation database combining various types of cameras with variations on the 3D point sampling parameters is built to evaluate different paths and their impact on the calibration. For every combination, we calibrate the camera and estimate the reprojection error statistics from the previous section as a proxy for the uncertainty and reliability of the resulting calibration.

In order to build the aforementioned database, an experimental design technique is used to model 5000 different cameras by changing in a continuous way the focal length, the image dimensions, the camera elevation and orientation. The distortion is also varied for these cameras between two levels: pinhole or medium distortion. This technique must handle continuous and discrete variables. Since few cameras have a field of view angle equal to 180 or 20 degrees, a small ratio of points should be sampled at the design space extremities while the design space interior should be highly represented. Based on these properties, a Latin Hypercube design was selected to sample the design space made of the five factors (focal length, image width, camera elevation and orientation and distortion level) and create 5000 cameras [13].

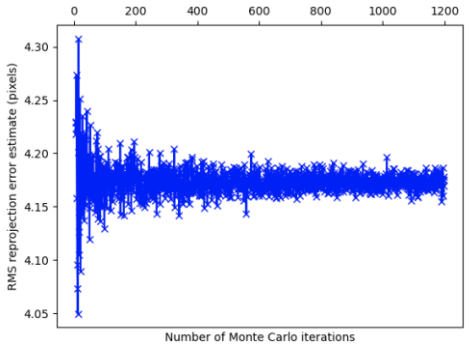

Figure 1: Convergence of the RMS reprojection error estimate with the number of Monte Carlo iterations

The resulting database was used in two different ways: 1) knowing some parameters, the influence of the other parameters can be plotted to highlight local optima, and 2) with little knowledge about the camera model, recommendations on the optimal sampling strategies can be provided, not only in terms of reprojection error but also in terms of robustness against measurement uncertainties. Figure 2 provides an overview of the process leading to the data injection in the database.

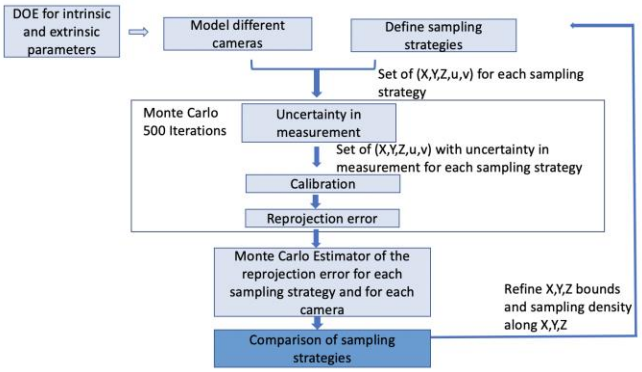

Figure 2: Data collection about calibration uncertainty for a large variety of cameras and sampling paths

III. Experimental Setup

The goal of the methodology defined in section II is to estimate the calibration uncertainty resulting from a given path and the localization and detection uncertainties. To do so, the model of the uncertainty of the drone localization on images must be estimated. This uncertainty is mainly due to small drone movements at sampled points and the availability of a clear view of the drone on the video. The design of an experiment to estimate the localization uncertainty is presented in Section A. Section B presents the design of an experiment to evaluate the impact of 3D and 2D localization uncertainties and different drone paths on the calibration, using in part the results from the first experiment.

A. Drone detection methods and 2D localization accuracy

The first experiment was designed to compare two drone detection methods and to estimate the uncertainty associated with the 2D point localization. Simulations with different cameras, different environments and different drone paths using the Robot Operating System (ROS), Gazebo and the Parrot Bebop 2 simulated drone (which is part of the Rotors package of ROS) are used for the estimation [14]. Each simulation is used to gather 3D and matching 2D key points. In these experiments, the drone flies in the camera field of view to waypoints whose GPS coordinates are the key 3D points required for the calibration.

Then the camera video is used to detect the drone at these key points and extract its 2D pixel location, thus obtaining a set of 3D and 2D matching points. To simplify the correspondence problem, in this work the drone maintains position stationary for a specified time interval at waypoints. This solution enables a convenient correspondence between 3D and 2D points but increases the drone mission time. An alternative solution that relies on GPS and video time synchronization would enable a correspondence without stopping at waypoints. The 3D and 2D points are used to calibrate the camera and the reprojection errors are computed to evaluate the calibration accuracy. This experiment first compares the impact of two drone detection methods on the calibration accuracy. In the first case, the drone is manually detected by clicking it in the image. In the second case, a marker is attached to the simulated drone model and automatically detected in the camera frame. Figure 3 illustrates the drone design used for this second method. With this experiment, the accuracy of the 2D point sampling is estimated and is used as an input to the path evaluation experiment.

The simulations were implemented for two cameras, a pinhole camera and a camera that includes distortion. The camera parameters are provided in table 1. The world frame taken for this experiment is the Gazebo frame where the x and y axes define the ground plane and the z axis is vertical up.

Table 1: Cameras intrinsic and extrinsic parameters

Camera model	Pinhole camera	Camera with distortion
Focal length (pixel)	1110	1110
Image center coordinates (pixel)	(640, 480)	(640, 480)
Angle of rotation along y (degree)	30	30
Translation (m)	$T_x = 0.5$ $T_y = 0$ $T_z = 2$	$T_x = 0.5$ $T_y = 0$ $T_z = 2$
Radial distortion coefficient (m^{-2})	none	k_1=-0.25
Tangential distortion coefficient (m^{-1})	none	p_1=-28e-5 p_2= -5e-5

The drone path is constrained by the coverage of the field of view and simple trajectory requirements. In order to calibrate the camera, it is necessary to get 2D key points that cover most of the image [7] as the points close to the image center are not subject to the distortion in the same way as the points close to the image boundaries. In addition, using 3D key points from a unique plane might induce a bias when computing the camera parameters [6]. Consequently, the drone path should cover a maximum of the field of view while flying in several planes. A simple motion trajectory made of straight lines or circles is also important in order to reduce the flight time and cost [15, 16]. In order to satisfy the simple trajectory requirement and the field of view coverage

requirement, the trajectories involve the drone flying a back-and-forth motion in several planes contained in the camera field of view. As a final practical design constraint, the sampling height can only be covered up to points directly above the ground to avoid having the drone taking off and landing several times during the calibration. Two different paths providing different benefits were tested. First, one located between X=4m and X=6m and second, one located closer to the camera between X=3m and X=5m. The path closer to the camera covers a larger part of the height of the FOV; however, simulation results showed that the calibration is slightly more accurate for the path farther away from the camera. Figure 4 illustrates these paths. The camera is located on the left side at (0,0,2). The blue path represents the GPS location while the green path represents the marker center of gravity location. Figure 5 illustrates the image from the camera with the sampled points obtained using the first back-and-forth path.

These simulations provide a way to compare the impact of the drone detection methods on the calibration accuracy and to develop a model for the 2D localization uncertainty. Using this knowledge, an experiment was completed to evaluate the calibration uncertainty for a given path and the localization and detection uncertainties. This is described in section B.

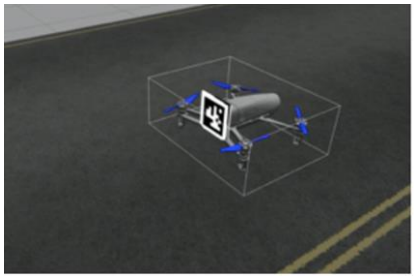

Figure 3: New drone design with a marker for a more accurate calibration

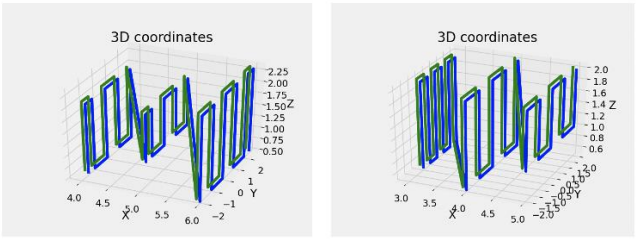

Figure 4: Marker path (green) and GPS path (blue) used for the calibration with ROS and Gazebo simulations

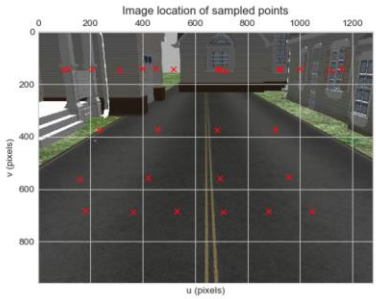

Figure 5: Image of the camera view obtained from Gazebo simulations and representation of the sampled points (red)

B. *Evaluation of sampling strategies*

The second experiment was designed to test several sampling strategies to determine their robustness for calibration across a large variety of cameras following the approach described in section II.

Based on the sources of uncertainty identified and expectations about real-world use with a drone equipped with a RTK GPS, the uncertainty in GPS, altimeter measurement and the drone location measurement in the image are included. The 3D localization uncertainty is modeled by a Gaussian distribution with zero mean, a 1.5-centimeter standard deviation along Z and a 1-centimeter standard deviation along X and Y [17]. Using the results from the first experiment, the drone location error was modeled by a Gaussian distribution of zero mean and 2-pixels standard deviation.

5000 different cameras were modeled by changing the focal length, the image dimensions, the distortion, the camera elevation and orientation. The focal length was varied between 2 millimeters and 15 millimeters, the image width was varied between 700 and 4,000 pixels and the image height was related to the width by a ratio of three quarters. The camera elevation was varied between 2 and 5 meters and the camera orientation was varied between zero (horizontal) and 90 (vertical) degrees. The distortion was varied discretely between two possible levels: no distortion for a pinhole camera model, and a radial and tangential distortion modeled by the Brown equations [18].

The camera models were selected using a Latin Hypercube experimental design and used to evaluate different sampling strategies and provide guidance about the points to sample for an accurate drone-based calibration.

The baseline sampling for obtaining the 3D key points is inspired by the path defined in the first experiment while adding more points along Z. This sampling is made of points located every meter along X and Y and every 50 centimeters along Z, where X, Y and Z define the world frame. The cameras are located at X and Y equal 0 and at various elevations. A limit for the distance from the camera to the drone was taken equal to 8 meters along the X axis and 3 meters on each side of the camera along the Y axis. These limits were chosen based on the Gazebo and ROS simulations where the marker was not systematically detected once the drone flew above these limits.

Several samplings are derived from this initial sampling by modifying the density of samples along X, Y and Z. For each sampling strategy, each camera is calibrated using the 3D points obtained from the sampling, their 2D location computed using the camera parameters and the addition of uncertainty for measurement errors.

Once the sampling densities along X, Y and Z are fixed, an additional set of simulations was run to compare a sampling closer to the camera to one farther away. Sampling closer to the camera covers a larger part of the image width but the impact of the GPS uncertainty decreases when sampling points farther away from the camera. Having fewer samples at the image edges might lead to a poorer model accuracy of the 3D-to-2D mapping at the image borders compared to a scenario where more points are available away from the optical axis. This, in turn, might lead to an increased reprojection error at those points and an increased RMS reprojection error. As a result, there is a tradeoff between

sampling farther away and closer to the camera. The simulations comparing the closer and farther samplings provide recommendations for the path sampling parameters.

IV. Experimental Results and Discussion

A. 2D location methods and modeling of 2D measurement uncertainty

The experiment investigating the calibration uncertainty using simulations in ROS and Gazebo compare two drone detection methods and build a model for the 2D point detection uncertainty. First, both a drone with a marker and one without a marker and a pinhole camera without distortion and a camera with distortion were tested. Figure 6 provides the results obtained from these simulations. All RMS reprojection errors are smaller than 3.3 pixels and adding a marker decreases the error by 24 percent on average. These results confirm that the choice of the detection method influences the calibration accuracy. The pixel location measurement uncertainty must be modeled to evaluate precisely the impact of different drone paths and location uncertainties on the calibration. The reprojection error obtained at sampled points with these simulations is used to estimate this model. A second set of simulations was created that allows modeling cameras and uncertainty in pixel location measurements, and computing calibration error distributions. Within these simulations, the uncertainty in the 2D points' locations is modeled using a Gaussian distribution of mean zero and standard deviation 2 pixels and the cameras used in the aforementioned Gazebo simulations are modeled. A graphic comparison of the reprojection error distributions provides a first element towards the validation of the model for the 2D measurement uncertainty. The reprojection error distributions obtained from the Gazebo experiments and the ones obtained from the second set of simulations are Gaussian in shape and they have qualitatively similar medians, as depicted in figure 7, with pinhole cameras on the two left columns and cameras with distortion on the two right columns. To complete the validation of the 2D measurement uncertainty model, a statistical hypothesis test was used to compare the means. This involved testing the null hypothesis that the two samples have the same mean with a two-sided t-test [19]. The two samples refer to the sample obtained through the Gazebo experiment and the sample obtained through the second set of simulations for the same camera. The p-value obtained from this test was equal to 0.64 which is larger than the chosen threshold of 0.10, therefore the null hypothesis is accepted. When combined with the qualitative shape comparison, this enables the validation of the model for the 2D points location uncertainty for this use.

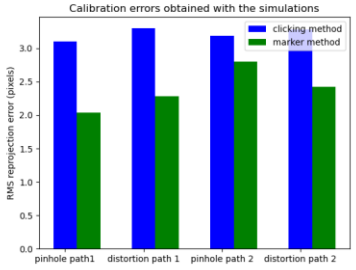

Figure 6: ROS and Gazebo simulation results and comparison of manual and automated detection methods

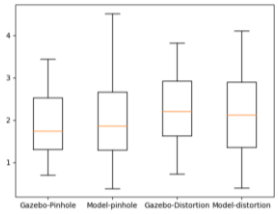

Figure 7: Reprojection error distributions obtained using Gazebo and the Gaussian model providing a first element for the validation of the uncertainty model

Summarizing this experiment: first, when comparing the two drone detection methods, we observe, as expected, that adding a marker on the drone improves the calibration accuracy. This confirms that the detection method has an impact on the calibration and modeling its uncertainty is necessary to accurately estimate the calibration uncertainty.

Secondly, and more importantly, we validated the model of the influence of the 2D measurement uncertainty on the calibration uncertainty for use in the next experiment. This model is a key enabler to accurately represent the calibration uncertainty for different paths while including localization uncertainties as described in sections II.B and II.C.

Finally, when considering the practical deployment of the drone-based calibration approach, all RMS reprojection errors obtained are smaller than 3.3 pixels. The pixel error corresponds to a speed measurement error smaller than 1km/h when measurements are done with the aforementioned cameras. In terms of the general calibration approach using a drone, the simulation results show promise for actual use for calibrating a camera for speed-measurement applications.

B. Comparison of 2D localization methods and modeling 2D uncertainty

Experiment 2 models the uncertainty for the 2D key points' locations using the distribution obtained in the first experiment and includes the uncertainty for GPS and altimeter measurements. This experiment evaluates the impact of path sampling parameters on the calibration of a large diversity of cameras using the methodology described in sections II.B and II.C., leading to recommendations for the path sampling strategy.

The sampling parameters that are varied first are the sampling densities along Z, Y and X in the world frame defined in section III.B. First, three simulations with different sampling densities along Z were completed. Results demonstrated that for 98% of camera models, increasing the number of sampled Z-values from two values to three or four values did not improve the calibration accuracy. In addition to enabling good calibration, sampling two-Z values instead of three or four leads to a simpler drone trajectory.

A second set of simulations compared the impact of sampling step-lengths along Y equal to 50 centimeter and 1 meter. The results demonstrated that using a step-length of 1 meter leads to a better accuracy for 97% of cameras. Figure 8 illustrates the step-length choice for various focal lengths and image dimensions. On this graph, the contour value equals 1 when a step-length of 1 meter enables a better calibration and 2 if the preferred step length is 50 centimeters. This last step-length is advantageous for cameras with small focal lengths or large field of view angles.

Based on the simulations' results, it is recommended to

sample 3D points using a step-length equal to 1 meter along X and Y while sampling two Z-values. An exception exists for cameras with small focal length where a step length of 50 centimeters along Y is preferred. Figure 9 illustrates the impact of camera parameters on the calibration accuracy when the proposed sampling strategy is used. The top figure presents the contour plot of the RMS reprojection error for various image width and focal length values. The calibration accuracy decreases when the image width increases or the focal length increases. The bottom figure depicts the contour plot of the RMS error for various orientations and elevations of the camera. It can be seen that the calibration accuracy is poorer for cameras with small elevation and large orientation angles (near vertical). For these configurations, the drone can only fly close to the camera. This causes the GPS uncertainty to have an important impact. This is depicted in Figure 10 where the impact of the GPS measurement uncertainty corresponds to the distance between the two curves and decreases when the maximum sampling distance increases. The bottom curve is obtained using 2D point location uncertainty only. This result is obtained for a camera with focal length of 1,000 pixels, image dimension of 1,200 pixels, rotation of 45 degrees and elevation of 4 meters.

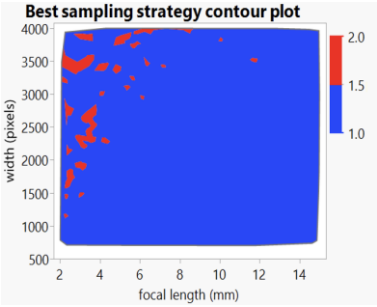

Figure 8: Comparison of sampling step-length along Y for various image width and focal length values

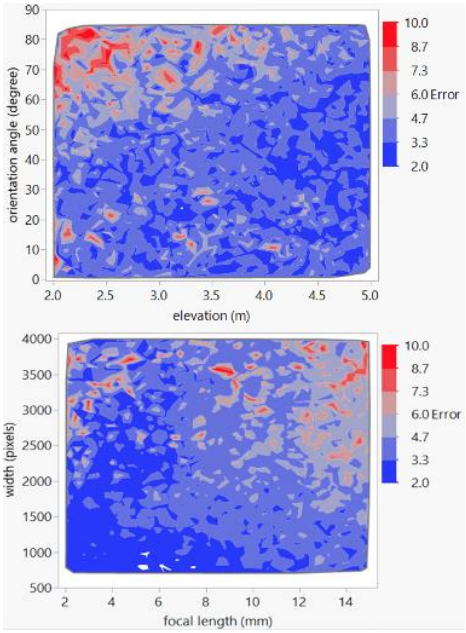

Figure 9: Variation of the RMS reprojection error for various camera orientations and elevations on the top and various image width and focal length values on the bottom

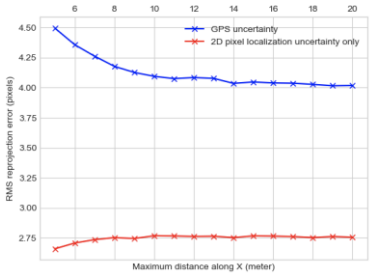

Figure 10: Impact on the calibration error of increasing the sampling distance from the camera

Based on these observations, another set of simulations was used to compare a sampling close to the camera to one farther away from the camera. The first simulation used a sampling where values along the X-axis varied between 0 and 8 meters. In a second simulation X-values varied between 0 and 4 meters and the third simulation used X-values between 4 and 8 meters.

According to the simulation's results, 79 percent of cameras have better calibration accuracy when using a sampling farther away from the camera. The remaining 21 percent of cameras have common characteristics; they have extreme field of view angle values. Consequently, for most cameras, it is recommended to sample points farther from the camera, at a distance larger than 4 meters away to ensure a good calibration in spite of the GPS and altimeter uncertainties. An exception exists for cameras with very large or very small field of view angles. The results also demonstrated that sampling farther away from the camera reduces the average of the RMS reprojection error on all cameras by 38 percent, leading to an average RMS error of 4 pixels.

Coming back to the application we considered in the introduction, this reprojection error corresponds to a speed measurement error smaller than 0.5km/h when measuring the speed of a vehicle 15 meters away using a pinhole camera of focal length 900 pixels. It also corresponds to a measurement error of 8 centimeters while locating an obstacle 15 meters away from the camera. As such, it can be concluded that the proposed sampling strategy enables the calibration of cameras within a reasonable accuracy for speed measurement and UAM obstacle location applications.

V. Conclusion and Future Work

The paper introduced a calibration approach that can be applied to any area or volume size covered by the field of view of a camera, and thus is adapted for hard-to-reach cameras. The calibration approach relies on the use of a drone to collect data required for the calibration. To define a flight path allowing for the calibration of cameras, a methodology is derived to evaluate the impact on the calibration accuracy of path parameters and uncertainty in localization and drone detection. This methodology is applied to evaluate different sampling strategies for a large variety of cameras resulting in recommendations about robust path parameters. The choice of the drone path and the drone detection method have a significant impact on the calibration accuracy. Future work aims at improving the calibration accuracy by autonomous exploration of the field of view and replacing the marker by a LED. The method will also be tested in a real setting.

REFERENCES

[1] A. Albarelli , E. Rodola and A. Torsello, "Robust Camera Calibration using Inaccurate Targets," in *British Machine Vision Conference*, 2010.

[2] N. Borlin and P. Grussenmeyer, "Camera calibration using the damped bundle adjustment toolbox," *ISPRS Annals of the Photogrammetry, Remote Sensing and Spatial Information Sciences,* 2014.

[3] J. Heikkila and O. Silven, "A four-step camera calibration procedure with implicit image correction," in *IEEE Computer Society Conference on Computer Vision and Pattern Recognition*, 1997.

[4] IHS Markit, "Video Surveillance: new installed base methodoloogy yields revealing results," 2019. [Online]. Available: https://ihsmarkit.com/pdf/IHS-Video-surveillance-installed-base(2)_227038110913052132.pdf. [Accessed 2020].

[5] Z. Zhang, "Camera calibration with one-dimensional objects," *IEEE Transactions on Pattern Analysis and Machine Intelligence,* vol. 26, pp. pp. 882-899, 2004.

[6] Z. Zhang, "A flexible new technique for camera calibration," *IEEE Transactions on Pattern Analysis and Machine Intelligence,* vol. 22, pp. 1330-1334, 2000.

[7] X. Zhang, C. Wang, Y. Fang and H. Lu, "Global homography calibration for monocular vision-based pose measurement of mobile robots," *International Journal of Intelligent Robotics and Applications,* 2017.

[8] S. Ramalingam, P. Sturm and S. Lodha, "Towards complete generic camera calibration," in *IEEE Computer Society Conference on Computer Vision and Pattern Recognition*, 2005.

[9] O. Faugeras, Q. Luong and S. Maybank, "Camera self-calibration: Theory and experiments," in *European Conference on Computer Vision*, 1992.

[10] E. Hemayed, "A survey of camera self-calibration," in *IEEE Conference on Advanced Video and Signal Based Surveillance*, 2003.

[11] R. Haralick, "Propagating covariance in computer vision," in *International Conference on Pattern Recognition*.

[12] A. Ortega , R. Galego, R. Ferreira and A. Bernardino, "Estimation of camera calibration uncertainty using LIDAR data," in *European Conference on Mobile Robots (ECMR)*, 2013.

[13] J. Barros, M. Kirby and D. Mavris, "Impact of sampling technique selection on the creation of response surface models," *SAE transactions,* 2004.

[14] F. Furrer, M. Burri, M. Achtelik and R. Siegwart, "Rotors - A modular gazebo MAV Simulator Framework," in *Robot Operating System (ROS): The Complete Reference*.

[15] E. Galceran and M. Carreras, "A survey on coverage path planning for robotics," *Robotics and Autonomous Systems,* 2013.

[16] T. Cabreira, L. Brisolara and P. Ferreira, "Survey on Coverage Path Planning with Unmanned Aerial Vehicles," *drones,* 2019.

[17] Y. Feng and J. Wang, "GPS RTK Performance Characteristics and Analysis," *Journal of Global Positioning Systems,* 2008.

[18] D. Brown, "Close-Range Camera Calibration".

[19] A. Hayter and A. Hayter, "Chapter 8: Inferences on a population mean," in *Probability and Statistics for Engineers and Scientists*, Brooks, Cole, 2006.